Cerebral Cortex, May 2021;31: 2639–2652

doi: 10.1093/cercor/bhaa380
Advance Access Publication Date: 31 December 2020
Original Article

ORIGINAL ARTICLE

Altered Inferior Parietal Functional Connectivity is Correlated with Praxis and Social Skill Performance in Children with Autism Spectrum Disorder

Nicholas F. Wymbs[1,2], Mary Beth Nebel[1,2], Joshua B. Ewen[2,3,4] and Stewart H. Mostofsky[1,2,5]

[1]Center for Neurodevelopmental and Imaging Research, Kennedy Krieger Institute, Baltimore, MD 21205, USA, [2]Department of Neurology, Johns Hopkins University School of Medicine, Baltimore, MD 21205, USA, [3]Department of Neurology and Developmental Medicine, Kennedy Krieger Institute, Baltimore, MD 21205, USA, [4]Department of Psychological and Brain Sciences, Johns Hopkins University, Baltimore, MD 21205, USA and [5]Department of Psychiatry and Behavioral Sciences, Johns Hopkins University School of Medicine, Baltimore, MD 21205, USA

Address correspondence to Stewart H. Mostofsky, Kennedy Krieger Institute, Center for Neurodevelopmental and Imaging Research, 716 North Broadway, 3rd Floor Baltimore, MD 21205, USA. Email: mostofsky@kennedykrieger.edu.

Abstract

Children with autism spectrum disorder (ASD) have difficulties perceiving and producing skilled gestures, or praxis. The inferior parietal lobule (IPL) is crucial to praxis acquisition and expression, yet how IPL connectivity contributes to autism-associated impairments in praxis as well as social-communicative skill remains unclear. Using resting-state functional magnetic resonance imaging, we applied independent component analysis to test how IPL connectivity relates to praxis and social-communicative skills in children with and without ASD. Across all children (with/without ASD), praxis positively correlated with connectivity of left posterior-IPL with the left dorsal premotor cortex and with the bilateral posterior/medial parietal cortex. Praxis also correlated with connectivity of right central-IPL connectivity with the left intraparietal sulcus and medial parietal lobe. Further, in children with ASD, poorer praxis and social-communicative skills both correlated with weaker right central-IPL connectivity with the left cerebellum, posterior cingulate, and right dorsal premotor cortex. Our findings suggest that IPL connectivity is linked to praxis development, that contributions arise bilaterally, and that right IPL connectivity is associated with impaired praxis and social-communicative skills in autism. The findings underscore the potential impact of IPL connectivity and impaired skill acquisition on the development of a range of social-communicative and motor functions during childhood, including autism-associated impairments.

Key words: connectivity, dyspraxia, gesture, ICA, motor skill

Introduction

Deficits in motor behavior are commonly observed in autism spectrum disorder (ASD) (DeMyer et al. 1972; Hallett et al. 1993; Teitelbaum et al. 1998; Mostofsky et al. 2006). Although not the defining features of the disorder, motor deficits are one of the earliest identifiable impairments in infants and toddlers that later receive diagnosis (Teitelbaum et al. 1998), with impairments in motor skill execution and learning linked to the core social and communicative skill deficits that define ASD (Dziuk et al. 2007; Dowell et al. 2009). Converging evidence suggests that children with ASD show impaired execution of skilled goal-directed actions (e.g., gestures) as well as impaired ability to cor-

rectly identify gestures when performed by others (Mostofsky et al. 2006; Dewey et al. 2007; Dowell et al. 2009; MacNeil and Mostofsky 2012), which is often identified as a developmental dyspraxia in the context of autism.

In individuals with ASD, developmental dyspraxia has been studied by examining the ability to perform gestures in response to verbal command, to imitation, and with tool use, with multiple published studies revealing children with ASD show broad-based praxis impairment across all three domains (Mostofsky et al. 2006; Dowell et al. 2009; Nebel et al. 2016). There is evidence suggesting that dyspraxia may be particular to ASD, with performance impaired in comparison to children with developmental coordination disorder and attention-deficit hyperactivity disorder (ADHD), as well as typically developing (TD) populations (MacNeil and Mostofsky 2012). Further, multiple studies of ASD have found a significant correlation of dyspraxia with measures of the core social-communicative features of ASD (Dziuk et al. 2007; Dowell et al. 2009), highlighting the possibility that abnormalities in neural circuits that underlie development of motor skills may more broadly contribute to impaired development of similar perceptual-action models necessary to development of social and communicative skills (Mostofsky and Ewen 2011). Despite this, the neural basis for praxis in children with ASD remains understudied.

Expression of praxis involves the dynamic interplay across a wide-ranging set of prefrontal, premotor, and parietal cortical regions (Johnson-Frey et al. 2005; Kroliczak and Frey 2009). Among these, the left inferior parietal lobule (IPL) has been consistently shown to have a key role in the representation of motor skills (Choi et al. 2001; Johnson-Frey et al. 2005; Hermsdorfer et al. 2007; Bohlhalter et al. 2009). Left IPL lesions from ischemic stroke are commonly linked to ideomotor apraxia (IMA), which is characterized by the impaired ability to perform motor skills on command or through imitation, with absence of a primary impairment in motor dexterity or a primary sensory defect (Heilman and Gonzalez Rothi 2003). Of the multiple subtypes of apraxia involving upper extremity movement, IMA largely concerns a disrupted integration of motor content that specifies cognitive and visuospatial features pertaining to familiar actions. For instance, IMA patients show particular sensitivity during tasks that involve pantomime gesture of familiar actions, in which case patients are tested on their ability to retrieve spatiotemporal kinematic and representational components of familiar actions, in the absence of actual tools or objects used (Leiguarda and Marsden 2000; Buxbaum et al. 2014).

Similarly, in neurotypical adults, neuroimaging research has consistently identified the left IPL as part of a praxis network, which includes other parietal, temporal, and frontal neocortical regions involved in representational and production-related control of sequential movements for skilled action (Johnson-Frey et al. 2005; Kroliczak and Frey 2009). The left IPL has been particularly emphasized with tasks involving the dexterous manipulation of the upper limb and fingers for the production of tool-related and communicative gestures (Bohlhalter et al. 2009; Kroliczak and Frey 2009). Further, recent evidence from both human (Wiestler and Diedrichsen 2013; Wymbs and Grafton 2015) and nonhuman primates (Quallo et al. 2009) suggests that the left IPL is also involved in the formation of skill-specific representations during skill learning. Evidence (Quallo et al. 2009; Wiestler and Diedrichsen 2013; Wymbs and Grafton 2015) and theory (Desmurget and Grafton 2000; Mostofsky and Ewen 2011) therefore suggest that the left IPL is important for the expression of forward action models, which contribute by means of rapid online correction during movement to avoid costly feedback-driven correction. As seen in IMA patients, forward action models can be disrupted through lesions to the IPL, which is densely connected within the ventro-dorsal processing stream. The ventro-dorsal pathway, running parallel to the dorso-dorsal processing stream, connects the posterior temporal cortex with the rostral cortical regions including the IPL and ventral premotor cortex and is believed to support the processing of everyday action representations or long-term memories of action (Binkofski and Buxbaum 2013). For instance, IM patients show the strongest impairment when online control is restricted, such as blindfolding to remove visual feedback during gesture or other more elemental movements, such as with reach to grasp (Buxbaum and Randerath 2018). Further, other high-level action processes rely on functional communication with the IPL, including motor imagery (Hardwick et al. 2018), action intention (Desmurget and Sirigu 2012), and action understanding (Rizzolatti and Rozzi 2018). Given these self-other processes, the IPL may also extend beyond actions identified as "motor skills," and considering that the IPL is heavily involved in social cognition (Igelström and Graziano 2017), it may support the development of social skills, including theory of mind and empathy (Mostofsky and Ewen 2011).

Connecting action and social modes of cognition, the IPL is a key node within the action observation network (AON), a network that is hypothesized to support imitation behavior, and, when compromised, may lead to impairments in core social and communicative features in ASD (Oberman and Ramachandran 2007). To understand how deficits of imitation and social-communicative function in children with ASD may be related to visuomotor integration connectivity, our group recently evaluated resting-state functional magnetic resonance imaging (rsfMRI) functional connectivity between visual and somatomotor networks in the context of measures designed to assess imitation and social-communicative behaviors (Nebel et al. 2016). Using independent components analysis (ICA) to isolate visual and somatomotor functional networks, we found that children with ASD show greater asynchrony between lateral visual and upper limb somatomotor networks relative to TD children and that greater asynchrony in children with ASD was correlated with poorer social-communicative skill. Critically, visual-somatomotor synchrony was correlated with praxis performance in TD children, but a similar relationship was not observed in the ASD group, possibly because children with ASD rely on alternate circuitry for praxis.

The involvement of the IPL in the integration of cognitive and sensorimotor information is further informed by the diverse structural and functional connectivity of the IPL with cortical (for review, Caspers and Zilles 2018) and subcortical regions (Clower et al. 2005; Prevosto et al. 2010; Caspers and Zilles 2018). Additionally, detailed tractography of IPL subregions reveals a hub-like structural architecture with diversity in connectivity throughout the cortex, with anterior–posterior gradient showing a transition from spatial-sensorimotor to polymodal association cortex (Caspers et al. 2011). A multimodal architecture is further echoed through evidence from functional connectivity showing that the IPL is imbedded in multiple resting-state MRI networks, with particular convergence on default mode and frontoparietal control networks (DMN, FPN, respectively) (Buckner et al. 2008; Corbetta et al. 2008; Vincent et al. 2008; Andrews-Hanna et al. 2010; Parlatini et al. 2017). These networks are consistently linked with core features of ASD, with the DMN involved in self-referential processing and social cognition (Buckner et al.

2008; Andrews-Hanna et al. 2010), and the FPN involved in task-directed cognitive control (Corbetta et al. 2008).

The diversity of IPL functional connectivity within whole-brain resting-state networks is related in part to regional subnetworks imbedded within the IPL (Igelström et al. 2015, 2017). Igelström et al. (2017) examined the organization and cerebellar connectivity of the temporoparietal junction (TPJ), an area located within the IPL that is involved in social cognition, both in neurotypical adolescents and in those with ASD. Using a constrained ICA approach to localize intrinsic TPJ subregions, they found reduced connectivity between a right dorsal TPJ (TPJd) subregion and the left cerebellum Crus II for the ASD adolescents. This result raises the possibility that within functional hubs, such as the IPL, select subregions with abnormal connectivity profiles may contribute to higher level cognitive deficits of praxis and social skills as consistently observed in children with ASD. Yet to date, the behavioral significance of IPL subregions has not been examined in the context of ASD.

To address this gap in knowledge about associations between IPL connectivity and skilled behaviors (e.g., motor, social, communication) in autism, we implemented a constrained ICA analysis of the IPL to investigate subregion functional connectivity as it relates to praxis and social skills in children, including children with ASD. This method is well suited for identifying overlapping but distinct patterns of connectivity within regions that show complex patterns of functional connectivity and provides a sensitive means to understand shared and divergent connectivity maps to distal cortical and subcortical targets for ASD and neurotypical children. The following hypothesis were made: (1) using a sample that included both ASD and TD children to provide a wider distribution of praxis, connectivity strength between the IPL and primary and secondary premotor regions would positively correlate with praxis; (2) consistent with prior published findings (Mostofsky et al. 2006; Dziuk et al. 2007; Nebel et al. 2016), children with ASD would show significantly worse praxis relative to TD children and that among children with ASD, this impaired praxis would be related to long-range IPL connectivity with other sensorimotor areas; and (3) the expression of social and motor skills would be similarly related to reduced IPL connectivity in children with ASD.

Materials and Methods

One-hundred and thirty-nine children (8–12 years old) volunteered with informed consent, confirmed by written assent from the participant and their legal guardian, for procedures approved by the Johns Hopkins Institutional Review Board in accordance to the guidelines specified by the Declaration of Helsinki. Of these, 70 children had high-functioning ASD and 69 were TD children. Each participant visited the Kennedy Krieger Institute on two occasions, with 2 weeks being the average time between visits and never exceeding 6 months. See Table 1 for details on demographics and behavior.

Children with ASD met DSM-IV or DSM-V criteria as confirmed using the Autism Diagnostic Observation Schedule-Generic (ADOS-G) and the Autism Diagnostic Interview-Revised (ADI-R). Diagnosis was confirmed by a child neurologist with over two decades of clinical experience (S.H.M.). Children were excluded if they had an identifiable genetic cause for ASD, documented prenatal/perinatal insult, or other neurological disorder including epilepsy as determined during the initial phone screening with parental guardian. TD children were excluded if they had a first-degree relative with ASD, or if responses to the Diagnostic Interview for Children (DICA-IV; Welner et al. 1987) indicated history of a psychiatric disorder. ASD and TD children were excluded if their full-scale IQ was below 80 on the Wechsler Intelligence Scale for Children IV or V (WISC-IV: $n = 134$; WISC-V: $n = 5$) but were still eligible if they scored above 80 on either the Verbal Comprehension Index or the Perceptual Reasoning Index.

Social-communicative behavior relevant to ASD diagnosis was assessed using the Social Responsiveness Scale (SRS, $n = 31$; SRS-2, $n = 34$; Constantino et al. 2003) questionnaire. The SRS measures the ability of a child to engage in appropriate reciprocal social interactions, by measuring the awareness, interpretation, response, and motivation to respond to the social and emotional cues of others. The SRS-generated social deficit severity index is consistent across raters (e.g., teachers and parents), and the raw score ranges from 0 to 195 with higher scores indicating more severe impairment.

Praxis was assessed by examining upper limb gesture performance using a version of the Florida Apraxia Battery (Gonzalez Rothi et al. 1997) that was modified for assessment of children (Mostofsky et al. 2006). The exam evaluated gesture performance across three domains: (1) gesture to a verbal command (GTC), (2) gesture imitation (GTI), and (3) manipulating a tool to demonstrate a gesture, or gesture with tool use (GTU). For GTC, gestures were either transitive (17 total, pantomimed use of an object such as striking a nail with a hammer), or were intransitive (8, e.g., making a fist or waving). For GTI, gestures either had semantic content (25 transitive/intransitive gestures) or were considered novel movements and free of semantic information (9 gestures). Two raters blind to diagnosis evaluated each videotaped session and scored each gesture as correct or incorrect, with a correct gesture being free of any of the 4 categories of error described below. At least 80% concurrence between raters was achieved for each assessment, and scores were averaged across raters. Briefly, error types followed the criteria set by Gonzalez Rothi et al. (1997): (1) spatial: internal or external configuration of gesture is inaccurate, (2) body-part-for-tool: using a body part instead of the tool for an action, (3) temporal: timing or sequence of action is incorrect, and (4) content/concretization: inappropriate use of mimed object or for transitive, performing gesture on a real object. Gestures could be labeled as showing more than one error type.

The performance for each section (GTC, GTI, GTU) was then summed to generate an overall cumulative score reflecting total percent correct across the gesture exam. The total score provided a metric of general praxis performance, collapsing across transitive and intransitive gestures, including those without semantic content. The total score was then entered as a covariate in the imaging analysis described below. See Mostofsky et al. (2006) and Dziuk et al. (2007) for additional details on this praxis assessment.

Prior to the acquisition of MRI data, children first participated in a mock-scanner session to prepare for the constraints and stimulation associated with a live scanning environment. MRI scans were acquired using a 3T Philips Achieva with either an 8-channel ($n = 79$, 156 time points; $n = 25$, 128 time points) or 32-channel head coil ($n = 35$, 156 time points). A single-shot, partially parallel, echo planar imaging sequence with sensitivity encoding was used to acquire 47 slices per repetition time (TR = 2500 ms, 3-mm axial slice thickness, no gap), echo time (TE) of 30 ms, flip angle of 70°, sensitivity encoding acceleration factor of 2, in-plane resolution of 3.05×3.15 mm (84×81 acquisition matrix), with individual slices collected in ascending

Table 1 Demographics and behavioral measures of praxis (values reflect mean and standard deviation, where applicable)

	Typically developing	Autism spectrum disorder	
Gender (M/F)	55/14	55/15	$X = 0.0179$, $P = 0.8937$
Age (years)	10.27 (1.15)	10.34 (1.47)	$T = 0.7442$, $P = 0.3270$
Handedness (L/mixed/R)	5/6/58	7/2/61	$X = 0.3009$, $P = 2.4019$
Race	15 black/7 multi/47 Caucasian	5 black/1 Asian/7 multi/55 Caucasian/3 unspecified	$X = 8.6207$, $P = 0.0713$
GAI	109.94 (12.87)	109.46 (14.37)	$T = 0.2094$, $P = 0.8344$
SES	49.90 (10.17)	52.51 (10.17)	$T = 1.4910$, $P = 0.1383$
Mean FD (mm)	0.22 (0.23)	0.30 (0.28)	$T = 0.6743$, $P = 0.5013$
Days between fMRI and FAB	16.07 (26.98)	9.55 (23.32)	$T = 1.5241$, $P = 0.1298$
ADOS total	N/A	13.43 (3.76)	
ADI (subscales a/b/c)		19.97/15.75/6.01 (5.75/4.64/2.04)	
SRS (total raw)	18.39 (9.97)	96.45 (26.40)	$T = 22.4705$, $P = 1.33 \times 10^{-26}$
Command % correct	69.94 (13.97)	53.51(18.13)	$T = 5.9769$, $P = 1.86 \times 10^{-8}$
Imitation % correct	72.25 (11.68)	55.04 (17.85)	$T = 6.7166$, $P = 4.56 \times 10^{-10}$
Tool use % correct	80.52 (11.40)	57.02 (20.61)	$T = 8.3034$, $P = 8.66 \times 10^{-14}$
Total praxis % correct	73.34 (10.65)	54.98 (16.93)	$T = 7.6410$, $P = 3.36 \times 10^{-12}$

order. The first 5 TRs (10 s) were excluded from acquisition to ensure magnetization stabilization. A high-resolution T1-weighted image of the whole brain was also acquired (TR = 8 ms; TE = 3.7 ms, 1-mm isotropic voxel resolution).

Data were preprocessed using FSL version 5.011 (Oxford Centre for Functional MRI of the Brain, Oxford, UK, http://www.fmrib.ox.ac.uk/fsl/). Anatomical images were normalized to Montreal Neurological Institute space using a 12-parameter affine transformation (FSL FLIRT). Functional images were corrected for head motion using rigid-body realignment by realigning each volume to the middle volume of the run. Functional volumes were adjusted for slice-timing offset according to standard ascending slice acquisition. The entire image time series was scaled using grand-mean intensity normalization. The transformation matrices to warp from native to standard space (MNI-152, 2 mm) were generated using boundary-based registration to align EPI images to the segmented native T1 and then to the MNI template. Transformed images were input to the functional connectivity analysis. To remove unwanted low-frequency drift, images were high-pass filtered at 0.01 Hz. Prior to artifact removal (FSL FIX), movement during the acquisition of fMRI was assessed using the frame-wise displacement (FD) metric (fsl_motion_outliers). Participants were excluded if greater that 2SD above the group mean FD (M = 0.29; SD = 0.22). Using these criteria, 11 children (7 ASD) were excluded from additional analysis. The remaining datasets were then subject to artifact removal (FSL FIX). After manual training of the FIX classifier on an independent set of 20 datasets, noise components were detected and the variance associated with these noise components was regressed from each functional time series.

Functionally independent subregions of the inferior parietal lobe (IPL) were identified at the group level with a constrained independent component analysis approach using the masked ICA Toolbox (mICA, Moher Alsady et al. 2016). Group analysis of IPL subregions began with the temporal concatenation of individual subject ($n = 128$, 1 scan/subject) preprocessed functional data. The group time series was then restricted to the IPL using a mask from the Jülich atlas provided with FSL software to demarcate the supramarginal (SMG) and angular (ANG) gyrii, including the intraparietal sulcus (IPS) (Fig. 1A). Constructed separately for the left and right hemispheres, selected regions with probabilistic threshold set at 25% included anterior IPL/supramarginal gyrus regions (rostral opercular: PFop; caudal opercular: PFcm; rostral: PFt; caudal: PF; mid-caudal: PFm), posterior IPL/angular gyrus regions (anterior: PGa; posterior: PGp), and regions within the IPS (hIP1, hIP2, hIP3). Please see Caspers et al. (2006, 2008) for additional details regarding the cytoarchitectonic localization of these regions. This approach avoids the inclusion of signal from outside the IPL region of interest by incorporation of spatial smoothing (6 mm FWHM) after the masking of the data. Separate constrained ICA analyses were performed for the left and right hemispheres. Estimation of model order for each hemisphere was performed over dimensions 2–10 using a reproducibility analysis approach. Spatial cross-correlation using split-half sampling identified model orders of 4 for the left IPL and 5 for the right IPL to be the most stable estimates. These model orders are consistent with previous temporal–parietal junction parcellations (including IPL) using rfMRI in neurotypical adults (Igelström et al. 2015, 2017). Using these model order estimates, the left and right IPL were parcellated based on z-transformations of the ICA results with voxels being allocated to a particular subdivision based on the component with the highest z-score for a given location.

Multivariate functional connectivity between each IPL subregion and the whole brain was assessed using dual regression as implemented in FSL (Fig. 1B). Dual regression uses the group-level ICA results to generate single-subject projections of each IC. The first regression stage used a general linear model with the spatial maps of the left and right IPL ICs as inputs to a design matrix. This step solved for the subject-specific time courses for each group-level IPL spatial map while controlling for the variance explained by the other spatial maps. The second regression step used the subject-specific IPL time courses in a design matrix to identify subject-specific whole-brain functional connectivity networks. The second-stage spatial regression was constrained by a gray matter tissue prior mask. The resulting maps provide a whole-brain measure of functional connectivity with each of the IPL subregion time courses for each participant.

To examine group differences in whole-brain functional connectivity associated with each IPL subregion, the resulting

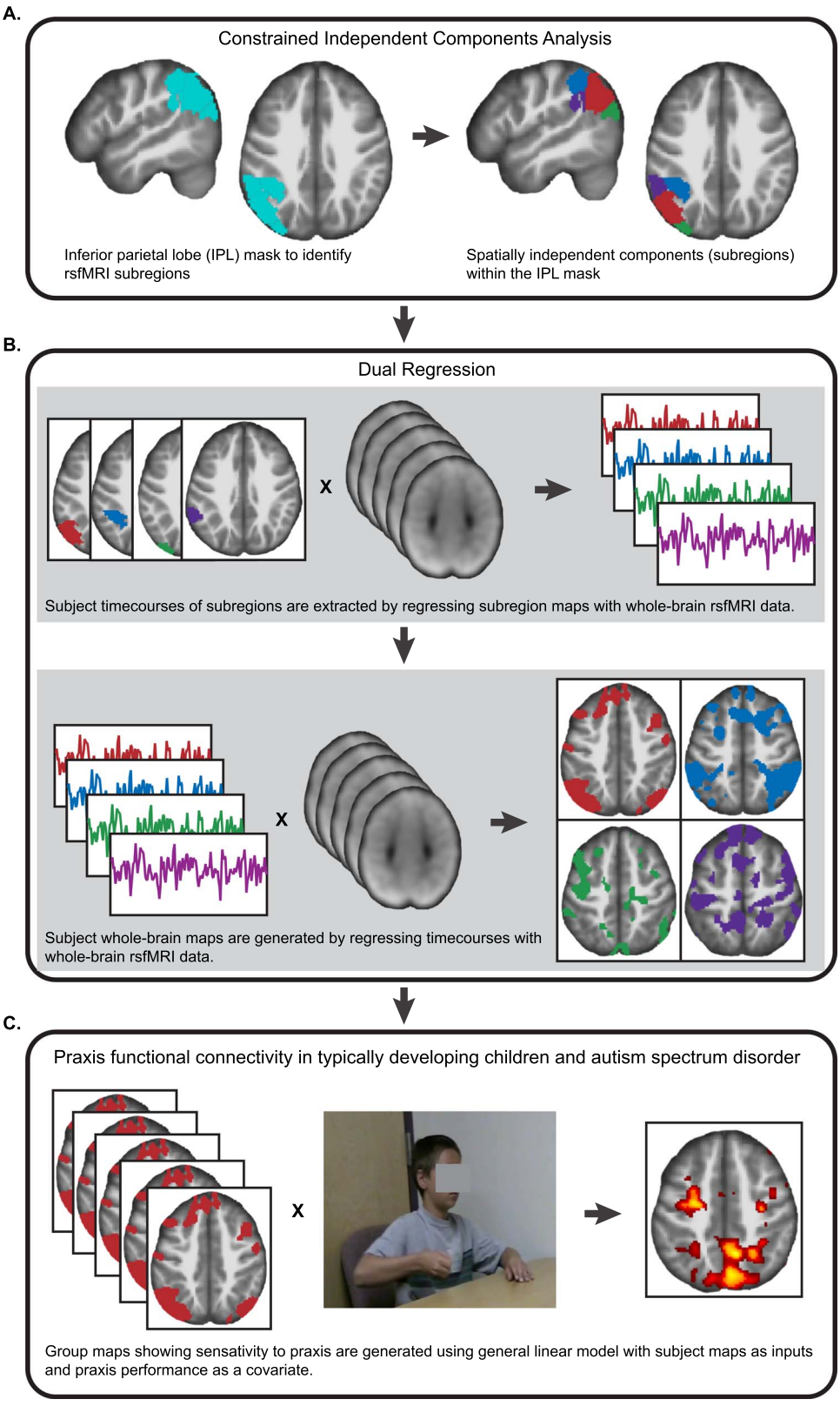

Figure 1. Schematic of the major analytical steps performed in the functional connectivity analysis of the IPL. (*A*) Using a pre-defined mask of the IPL, a constrained ICA approach was used to divide the IPL into subregions using resting state fMRI data sets ($n = 128$). (*B*) Dual regression was used to identify patterns of whole-brain functional connectivity arising from each IPL subregion. (*C*) To characterize the effect of IPL connectivity and praxis in TD children and ASD, whole-brain connectivity maps were entered into separate models for each IPL subregion, with praxis performance entered as a covariate of interest.

subject-specific spatial maps were analyzed with a multiple regression model using SPM12. A separate regression model was used for each IPL subregion. Age and handedness (categorical) were entered as covariates of non-interest in each model. Group effects were assessed with an initial cluster threshold of $P < 0.001$, Bonferroni corrected for the number of ICs (i.e., $P < 0.00011$), with reported effects FWE cluster-corrected for multiple comparisons at $P < 0.05$.

Three separate models were configured for each IPL subregion to address praxis and social skill hypotheses. First, to identify IPL functional connectivity in children related to praxis, the percent total correct metric from the FAB was entered in the regression model as a covariate of interest (Fig. 1C). A second regression model included an interaction term between clinical diagnosis and praxis percent total correct to identify anomalous connectivity in children with ASD as it is related to praxis. Finally, to test for overlapping functional connectivity patterns between praxis and social skill in children with ASD, covariates praxis percent total correct and SRS total raw were assessed using the global null conjunction option (Friston et al. 2005). For any given covariate result, we corrected for the influence of outlier data points from individual subjects by excluding clusters that contained subject means above 4SD from a group cluster mean.

Results

Behavioral Results

Children with ASD performed significantly fewer responses correctly than TD children on the gesture exam. For children with ASD, total praxis score ranged from 18 to 89% (mean 55%), whereas TD children ranged from 44 to 91% correct (mean 73%). A similar pattern in performance was reflected throughout the three sections of the exam (Table 1). Overall, statistical comparison of the total score and section-wise scores revealed that children with ASD made significantly more errors during the praxis: (see Table 1, total: $t = 7.64$, $P = 3.36 \times 10^{-12}$; GTC: $t = 5.9769$, $P = 1.86 \times 10^{-8}$, GTI: $t = 6.7166$, $P = 4.56 \times 10^{-10}$, GTU: $t = 8.3034$, $P = 8.66 \times 10^{-14}$).

Functional Connectivity of the IPL: Parcellation and Corresponding Whole-Brain Effects

We identified a functional parcellation of the IPL using constrained ICA at the group level for all participants (TD and ASD, $n = 128$) within a region covering the supramarginal and angular gyri (SMG and ANG, respectively), as well as the intraparietal sulcus (IPS), separately for each hemisphere. This approach resulted in the identification of subregions that are spatially consistent with previous functional and anatomical parcellations of the IPL (Fig. 2, see Caspers et al. 2006 Igelström et al. 2015 for IPL structural and functional parcellations, respectively). We identified subregions present in the right and left hemisphere as (1) a dorsal subregion (dIPL) overlapping with SMG (PF/PFm) that extended into the lateral bank of the IPS, (2) an anterior subregion (aIPL) that overlapped with more lateral SMG and extended into the parietal operculum (PF/PFm/PFcm/PFop), (3) a central subregion (cIPL) positioned at the transition zone between the SMG (PFm) and the anterior ANG (PGa), and (4) a posterior subregion (pIPL) that overlapped exclusively with the posterior ANG (PGp). We found an additional right hemisphere subregion that was positioned ventrally (vIPL) along the transition between the SMG (PFm) and anterior ANG (PGa).

Using dual-regression, we then examined whole-brain connectivity from each of the identified functional subregions (dIPL, aIPL, cIPL, vIPL, pIPL), first testing for group-level whole-brain networks (Fig. 3). This approach identified similar networks for right and left subregion pairs. The dIPL (Fig. 3, blue) connectivity map included regions of the superior parietal lobe (SPL), precuneus (PrC), posterior middle temporal gyrus (pMTG), medial and lateral premotor cortex extending into the middle and superior frontal gyri, and the lateral cerebellum (crus I/II). The pIPL (Fig. 3, green) connectivity map included medial and lateral SPL, PrC, medial and lateral premotor cortices, DLPFC extending to the inferior frontal gyrus (IFG), striate and extrastriate visual cortex, and cerebellum (lobules VI, VIII, crus I/II). The aIPL (Fig. 3, purple) connectivity profile consisted of sensory and sensorimotor regions, including connectivity to anterior IPL, medial and lateral SPL, medial and lateral premotor areas (extending to primary sensorimotor), anterior insula, lateral occipital areas, basal ganglia (head of caudate, posterior putamen), thalamus, anterior (lobule VI), and lateral cerebellum (Crus II). Whole-brain connectivity with the cIPL subnetwork (Fig. 3, red) included ANG, superior temporal sulcus (STS), PrC, medial prefrontal cortex, anterior and posterior cingulate (ACC and PCC, respectively), sensorimotor cortex, frontal operculum, and primary auditory cortex. Lastly, we observed a similar connectivity profile for the right hemisphere dominant vIPL (Fig. 3, orange), but with reduced activation in the frontal pole and sensorimotor cortex. Notably, we did not observe any significant group differences in connectivity for any of the IPL whole-brain networks (9 ICs), suggesting that TD and ASD children have similar IPL whole-brain functional organization. This is consistent with previous work that observed similar connectivity profiles of the temporoparietal junction (TPj), a region that included the IPL, in TD and ASD adolescents.

Association of IPL Network Connectivity with Praxis Across Diagnostic Groups (TD and ASD)

Praxis was significantly associated with functional connectivity involving multiple IPL subregions across all children. Consistent with known anatomical and functional relationship of the left IPL and praxis in adults, we found that greater gesture accuracy was related to increased connectivity of the left pIPL with bilateral cortical clusters of activation localized to the left dorsal premotor cortex (PMd), the left posterior intraparietal sulcus (pIPS), and multiple PrC foci located on the medial wall of the SPL (Fig. 4A, Table 2). We more closely observed that the PMd cluster was localized to the juncture of the superior frontal and precentral sulci and extended caudally to the primary motor cortex (M1, area 4p). The PrC cluster with the greatest spatial extent was localized to the right posterior PrC (smaller cluster in left PrC), extending along the superior aspect of the precuneal sulcus (PCS) and posteriorly to the anterior bank of the parieto-occiptal sulcus (POS). Position of this cluster is consistent with the human V6A homologue (Pitzalis et al. 2012). Additionally, we found another right hemisphere cluster positioned more anterior, between the PCS and marginal ramus of the cingulate sulcus.

Increased accuracy on praxis gestures was also associated with increased connectivity between the right cIPL subregion and the left SPL, as revealed through two clusters localized to

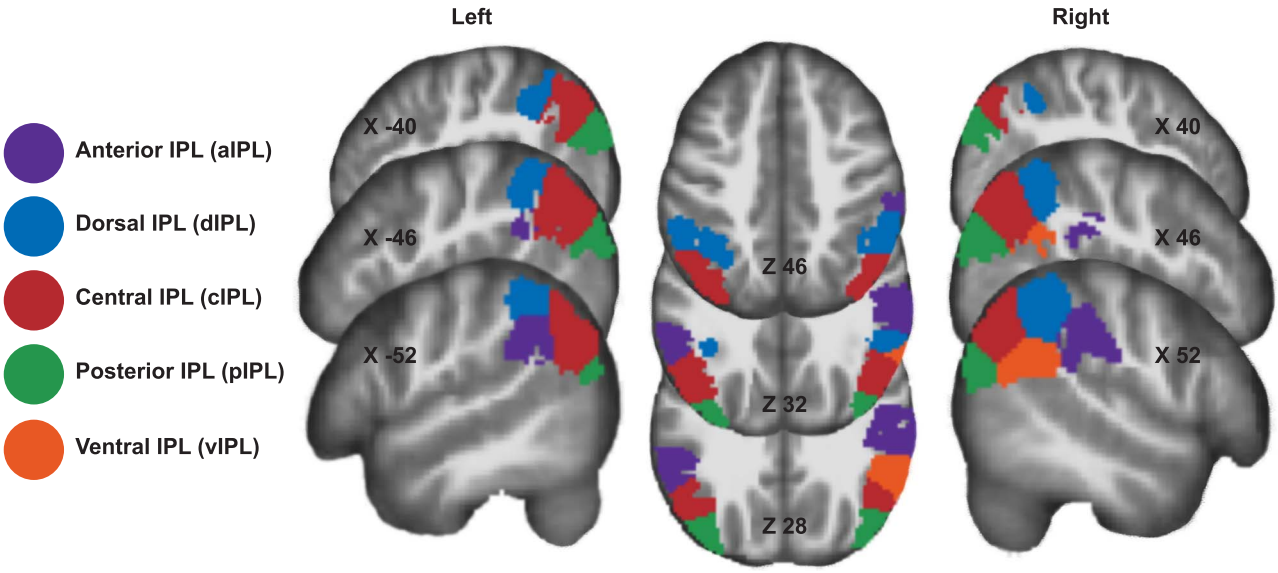

Figure 2. Parcellation of the IPL showing the subregions generated by constrained independent components analysis. Parcellation map reflects analyses for left and right hemispheres, with subregions colored to reflect similar spatial arrangement across hemisphere.

Table 2 IPL subregion—whole-brain connectivity effects of praxis

	MNI coordinates				
	x	y	z	Peak *T*	Voxels
Subregion: left pIPL					
Right superior parietal lobule	8	−74	46	5.05	296
Right precuneus	10	−54	48	4.92	144
Left angular gyrus	−28	−76	40	4.9	62
Left premotor cortex	−26	−12	50	4.82	203
Left precuneus	−6	−68	32	4.67	62
Subregion: right cIPL					
Left precuneus	−8	−60	50	6.05	192
Left superior parietal lobule/intra parietal sulcus	−34	−58	50	5.15	152
Subregion: right dIPL					
Right supramarginal gyrus	60	−26	28	5.46	98

lateral and medial (PrC) aspects of the SPL (Fig. 4B, Table 2). The lateral SPL cluster was positioned along the intraparietal sulcus (IPS) extending along the superior bank caudally from the primary intermediate sulcus of Jensen whereas the PrC cluster was localized within the PCS, and anteriorly towards the cingulate sulcus.

We additionally observed that increased connectivity of the right dIPL was related to stronger praxis performance (Fig. 4C, Table 2). Specifically, this pattern of increased connectivity in relation to praxis was observed between right dIPL and the right anterior supramarginal gyrus (SMG, Fig. 4C), with the cluster spanning the parietal operculum.

Further, we failed to observe any significant effect of diagnosis (ASD, TD) when comparing IPL connectivity with praxis performance. This lack of a statistical interaction suggests that connectivity profiles are generally similar between groups despite there being wide differences in praxis performance.

Table 3 IPL subregion—whole-brain connectivity conjunction of praxis and social skills

	MNI coordinates				
	x	y	z	Peak T	Voxels
Subregion: right cIPL					
Left cerebellum lobule VI	−28	−40	−34	4.44	66
Left posterior cingulate	−16	−42	48	3.7	115
Right superior frontal gyrus (rostral dorsal premotor cortex)	26	4	48	3.19	41

Relationship of IPL Connectivity to Praxis and Social Skill in Children with ASD

Using a conjunction analysis, we tested for overlap between IPL connectivity associated with motor and social skills in children with ASD. This approach revealed that the right cIPL subregion had similar connectivity relationships for both motor and social skills in autism (Fig. 5, Table 3) as measured by performance on the praxis exam and social skill ability rated by a parental guardian (SRS total score), respectively. The conjunction revealed that reduced connectivity with clusters in the right rostral PMd (PMdr), and the left anterior cerebellum (lobule VI) was associated with weaker praxis and social skills. Further, a third cluster was localized to the left retrosplenial cortex, including the ventral PrC and posterior cingulate cortex (PCC) (Fig. 5).

Discussion

Our primary aim was to understand if abnormalities in IPL functional connectivity were related to deficits in praxis and social skills commonly observed in school-aged children with ASD. We anticipated that reduced long-range connectivity from the IPL

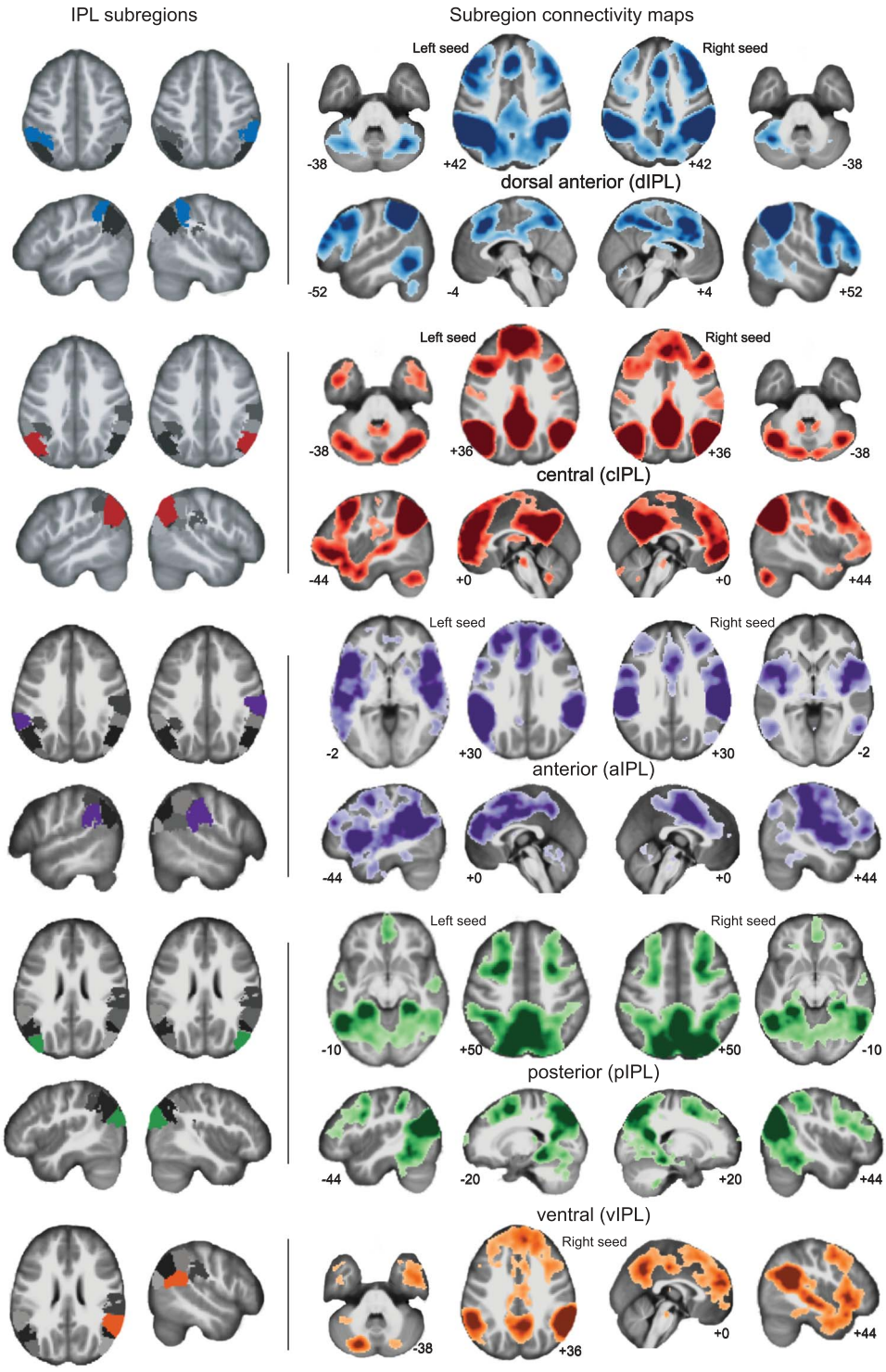

Figure 3. Subregions of the IPL and corresponding whole-brain networks observed in the TD and ASD dataset ($n = 128$). The position of the subregion is shown on the far left of the image, with images of the corresponding whole-brain connectivity shown on the center and rightmost panels. Darker shades reflect voxels of higher connectivity strength with the corresponding subregion ($P < 0.05$, FWE voxelwise correction).

and primary and secondary premotor regions would be linked to deficits in praxis performance and that similar connectivity reductions would be associated with poorer social skills. To address these hypotheses, we tested if differences in intrinsic functional connectivity (rsfMRI) are related to praxis and social-communicative skill in a wider dimensional sample of TD and ASD school-aged children (aged 8–12 years). Consistent with our hypotheses, we found that praxis performance across both

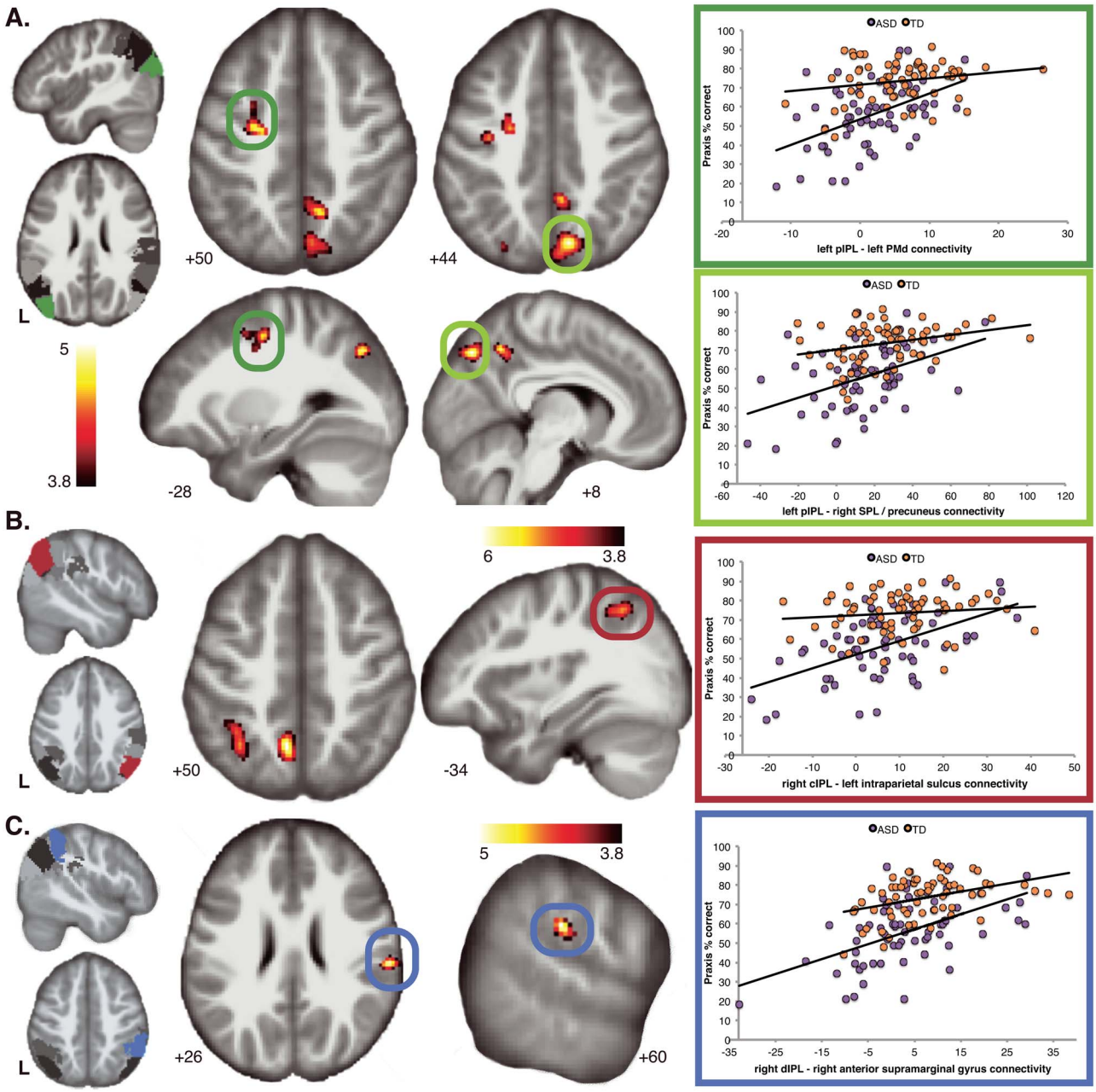

Figure 4. The relationship between IPL connectivity and praxis ability observed in a dimensional sample of TD children and children with ASD. (*A*) Regression of left pIPL whole-brain connectivity maps revealed significant relationship with praxis ability, with clusters isolated to the left dorsal premotor cortex (PMd, dark green circles), and right superior parietal cortex and precuneus (light green circles). (*B*) Analysis of right cIPL connectivity maps revealed that praxis performance was associated with increased connectivity of the IPS (dark red circles) and precuneus. (*C*) Analysis of right dorsal IPL (dIPL) connectivity maps revealed that praxis performance was correlated with connectivity of the right anterior supramarginal gyrus (dark blue circles). Right panels: coloring by diagnosis is to show the distribution of TD and ASD participants. Plots of effects illustrate the relationship between praxis ability and connectivity strength across the dimensional sample (TD + ASD). All maps are thresholded at $P < 0.05$, FWE cluster corrected.

ASD and TD children was associated with increased connectivity between distinct subregions of the IPL and primary and secondary premotor regions, which emerged bilaterally from both the right and left IPL. Consistent with several prior studies (Mostofsky et al. 2006; Dewey et al. 2007; Dziuk et al. 2007; Dowell et al. 2009), we found children showed impaired praxis performance compared with TD children. Further, we discovered that reduced right IPL (cIPL) functional connectivity was associated with impaired praxis performance, as well as impaired social skill, in children with ASD.

We found the IPL to fractionate into subregions (4 in left, 5 in right hemisphere), each with distinct patterns of connectivity with the rest of the brain. The subregion landscapes that we observed were comparable to IPL demarcations previously observed in functional connectivity approaches involving neurotypical young adults (Igelström et al. 2015), and anatomical

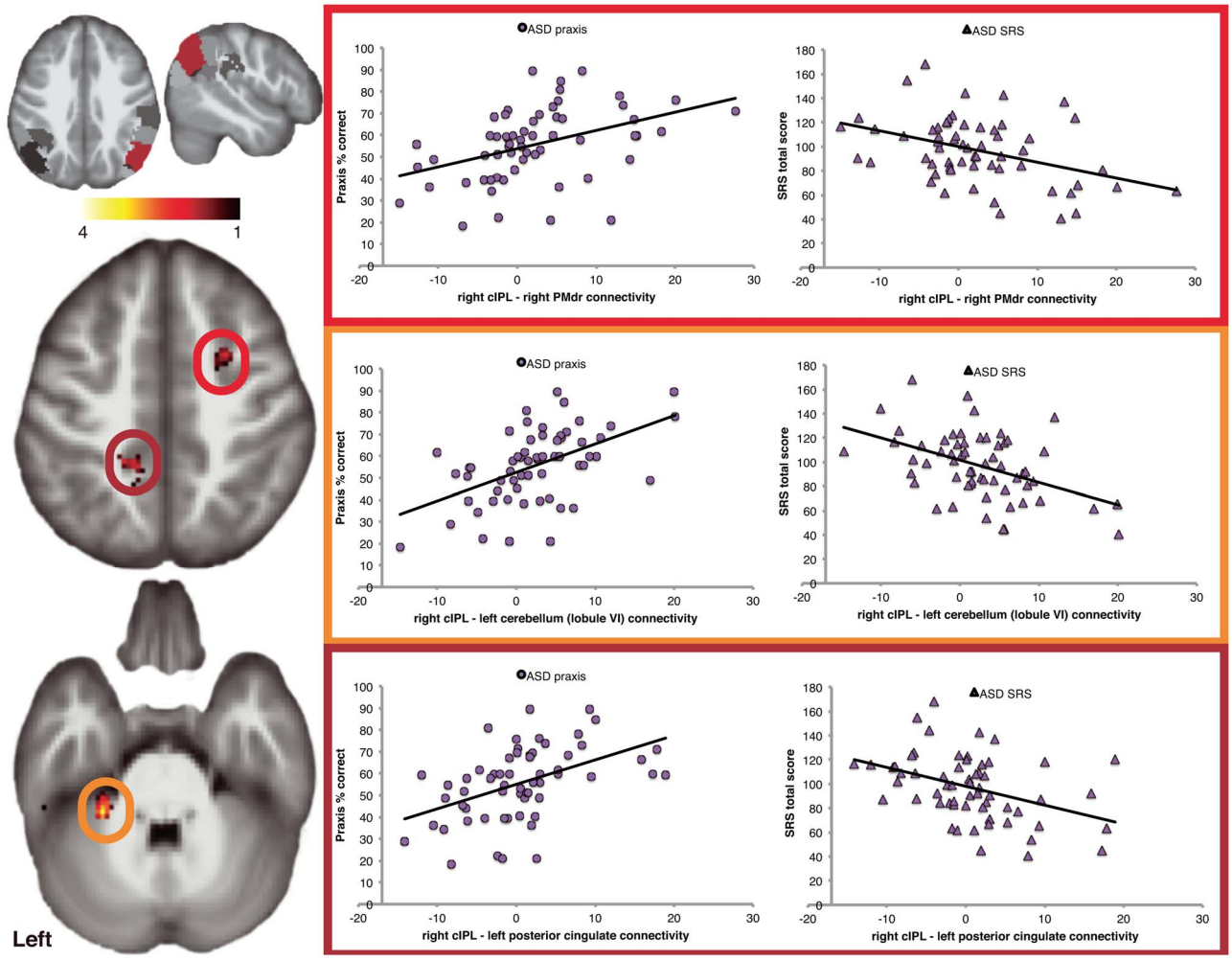

Figure 5. The relationship between IPL connectivity, praxis and social skills in children with ASD. Conjunction analysis revealed that right cIPL connectivity is similarly related to both motor and social skills, with increased connectivity to the left cerebellum (lobule VI, orange circle), posterior cingulate (dark red circle), and right rostral dorsal premotor cortex (bright red circle) associated with greater ability in social and praxis skills. Note that the SRS total score is inversely related to social skill ability, such that lower scores reflect greater social skill. All maps are thresholded at $P < 0.05$, FWE cluster corrected.

investigations (Caspers et al. 2006, 2008). Second, we found that particular subregions of the IPL demonstrated patterns of connectivity that tracked with praxis ability as measured across a dimensional sample consisting of both TD children and those with ASD. Using this approach, we found that children with stronger praxis tended to show greater connectivity between IPL subregions and distal brain regions commonly associated with motor skills. Third, we found that diverse patterns of IPL connectivity were associated not only with praxis motor skill, but also with social skill, in children with ASD. This suggests that anomalous development of the IPL may have a generalized impact on autism-associated impairments in acquisition of a broad-range of skilled behaviors, including those with motor and social composition.

Our results show that across a dimensional sample of children, praxis is supported by distinct patterns of IPL connectivity, such that connectivity with distal primary and secondary premotor regions was strongly linked to a child's performance on tasks requiring action knowledge. These findings illustrate the functional importance of IPL connectivity during childhood and serve to build upon an already rich understanding of the relationship between the IPL and action knowledge in adults (Hermsdorfer et al. 2007; Bohlhalter et al. 2009; Kroliczak and Frey 2009; Wiestler and Diedrichsen 2013; Wymbs and Grafton 2015; Buxbaum and Randerath 2018).

We observed that within a posterior subregion of the left IPL (pIPL) spanning posterior SMG and ANG, praxis ability tracks with increased connectivity with key areas of action representation, namely, left dorsal premotor (PMd), posterior parietal, and precuneus cortices. Connectivity between the left IPL and left PMd cortex is thought to be a cornerstone in motor skill representation (Kroliczak and Frey 2009; Buxbaum et al. 2014) including that of inverse models for action important for understanding actions as performed by others (Grafton 2009; Mostofsky and Ewen 2011). Association of praxis with left pIPL-precuneus is notable given that, like the IPL, the precuneus shows dense structural (Morecraft et al. 2003; Parvizi et al. 2006; Scheperjans et al. 2008) and functional connectivity with resting state networks (Buckner et al. 2008; Hagmann et al. 2008) highlighted in a diverse range of cognitive processes including

action representation, semantic memory, and social cognition (Hutchison et al. 2015).

Interestingly, we found that right IPL connectivity was associated with praxis ability, specifically right central IPL (cIPL) connectivity with the left intraparietal sulcus (IPS), extending into the SPL, and the left precuneus. These findings suggest that during child development, *both* the right and left IPL contribute to skill representation. These findings are consistent with evidence from neurotypical adults producing gestures with their non-dominant hand (Kroliczak et al. 2016; Buchwald et al. 2018), and further suggest the importance of interhemispheric (callosal) connectivity in development of skilled behaviors during childhood. Although it is far from conclusive, our findings argue for bilateral involvement of the IPL in motor skill representation during childhood and suggest the importance of cross-hemispheric integration of the IPL in the development of motor skills.

We additionally identified an autism-specific association, finding connectivity of the right cIPL to be strongly related to both motor and social skills in children with ASD. Decreased right cIPL connectivity to left cerebellum lobule VI, posterior cingulate, and right PMdr cortex was related to greater impairment in praxis and social skill ability. This finding is convergent with evidence from our research group (Dziuk et al. 2007; Dowell et al. 2009; Nebel et al. 2016) revealing an association of praxis and social skill ability in children with ASD. Moreover, this is consistent with the perspective that motor and social skills rely on overlapping neural networks and that abnormalities in motor skills, a phenotype that is illustrated early in development in ASD children, and thus may affect or are at least closely interrelated with the social-communicative skills that children build later in development (Mostofsky and Ewen 2011).

Reduced connectivity in right PMdr–cIPL overlaps with cortical territory comprising the dorsal frontoparietal network (dFPN), which is linked to executive control processing in a range of social and motor domains, including action emulation (Ptak et al. 2017), which pertains to the dynamic offline representation of kinematics and goals (Grafton 2009). In addition, the domain-general nature of this finding is supported by mounting evidence that networks involved in cognitive processes (e.g., FPN) demonstrate interactivity with other functional networks in response to task demands (Cole et al. 2013; Mattar et al. 2015) including social cognition (Dixon et al. 2018). Thus, the reduced long-range connectivity between the PMdr and cIPL may ultimately have adverse effects on skills that demand cognitive resources by weakening communication between functional networks.

The association of praxis and social skill with right cIPL-left anterior cerebellum (lobule VI) in children with ASD (Fig. 5A) highlights the potential contribution of cerebellar abnormalities to the pathophysiology of autism, with prior postmortem (Whitney et al. 2008; Skefos et al. 2014), behavioral (Haswell et al. 2009; Marko et al. 2015), and neuroimaging (Mostofsky et al. 2009; D'Mello et al. 2015) studies providing additional evidence for a role of the cerebellum in autism. Here, we show evidence that reduced parietal-cerebellar connectivity may contribute to a generalized impairment in skills acquired during early childhood in ASD. Interestingly, this finding is consistent with recent work using mouse and human models showing that cerebellar-parietal connectivity is both functionally and structurally altered, and is a key factor in the expression of autism-related behaviors (Stoodley et al. 2017). In this case, the investigators identified right Crus I—left IPL connectivity to be abnormal in human and mouse models, and that manipulation of mouse brain connectivity resulted in abnormal ASD-like social and repetitive use behaviors. Additionally, stimulation of the right Crus I—left IPL pathway rescued ASD-like social behaviors in their mouse model, which suggests that stimulation involving this pathway might serve to alleviate social skill challenges in children with ASD. Igelström et al. (2017) found a similar effect in adolescents with ASD, showing a reduction in functional connectivity with respect to controls, between the right dorsal TPJ subregion (located within the IPL) and the left Crus II. Our results extend these observed findings to show that a reduction in connectivity between the right IPL and left cerebellum is linked to a stronger ASD phenotype, in an earlier and more constrained developmental window, which may indicate a pathway that has a generalized effect on the acquisition and refinement of motor and communicative skills.

Notably, we observed that reduced right cIPL-left PCC connectivity was also associated with weaker praxis and social skills in children with ASD. The PCC is considered a hub within the DMN (Buckner et al. 2008), and due to strong mesial temporal structural connectivity, is linked to self-referential processes embedded in social skills, including autobiographical/episodic memory retrieval (Spreng et al. 2009), visuospatial mental imagery, and self-projection (Buckner et al. 2008). Aberrant PCC connectivity is associated with ASD (Leech and Sharp 2014; Lau et al. 2019) including the reduction in social skill performance (Lynch et al. 2013). We suggest that reduced IPL–PCC connectivity in children with ASD may affect the reconciliation and mapping of action and body knowledge, which may further disrupt the formation of praxis and social skill. Further studies are needed to address this possibility.

There are some limitations of our study that merit inquiry. Our results cannot speak to an evoked response of IPL praxis activity given that praxis was assessed outside of the scanner environment. Instead, our results highlight the latent functional pathways of the IPL and how these relate to praxis and social skill. Recent investigations are indeed making progress in this effort (e.g., McAuliffe et al. 2016), suggesting that acquisition pipelines that are more robust to motion artifact (e.g., fNIRS) or in conjunction with cutting-edge motion artifact computation (e.g., EEG/MEG) may provide the basis for praxis-related evoked response of the IPL. Another limitation was that we quantified praxis as an aggregate rating (percent correct) that was further aggregated across different gesture types. There is strong debate over what component of actions (e.g., kinematic, semantic) is represented within the left IPL (Bohlhalter et al. 2009; Kroliczak and Frey 2009; Buxbaum et al. 2014), but this topic is greatly underexplored children and remains a topic of future study. Lastly, we have limited insight regarding potential developmental effects of IPL connectivity and praxis because the chosen sample is confined to a single time point within a narrow range of school-aged children. Advances in neuroimaging in infancy and preschool children invite future efforts to examine the neurodevelopment of the IPL and how it may relate to the emergence of skills that are later impaired in children with ASD, which may lead to the development of early interventions that promote praxis and social skill in very young children at risk for autism.

Here, we observed that in school-aged children including those with ASD, there are multiple subnetworks of the IPL, arranged bilaterally, that show distinct patterns of intrinsic functional connectivity in support of praxis. Connectivity related to praxis was similarly observed in the left and right IPL,

which is somewhat surprising given the evidence of strong lateralization of praxis to the left IPL. The additional contribution of right IPL connectivity in this population of school-age children (with and without ASD) may be a consequence of ongoing development of association cortex, with yet undetermined (left) lateralization of praxis. Furthermore, our findings suggest that abnormalities in right IPL connectivity (specifically, right cIPL) in children with ASD may contribute to a generalized impairment of communicative skills, as we observed reduced connectivity linked to both praxis and social skills common to the ASD phenotype. These results highlight the potential wide-ranging impact that the IPL has on the development of motor skills and how aberrant IPL connectivity in ASD may contribute to challenges in the expression of motor skills applied to social-communicative interaction.

Notes

Conflict of interest: None declared.

Funding

Autism Speaks, National Institute of Mental Health (R01 MH106564, R01 MH113652, K01 MH109766); National Institute of Neurological Disorders and Stroke (R01 NS048527); Eunice Kennedy Shriver National Institutes of Child Health and Human Development (U54 HD079123); National Center for Research Resources Clinical and Translational Science Awards Program (UL RR025005); National Institute of Biomedical Imaging and Bioengineering (P54 EB15909).

References

Andrews-Hanna JR, Reidler JS, Sepulcre J, Poulin R, Buckner RL. 2010. Functional-anatomic fractionation of the brain's default network. *Neuron*. 65:550–562.

Binkofski F, Buxbaum LJ. 2013. Two action systems in the human brain. *Brain Lang*. 127:222–229.

Bohlhalter S, Hattori N, Wheaton L, Fridman E, Shamim EA, Garraux G, Hallett M. 2009. Gesture subtype-dependent left lateralization of praxis planning: an event-related fMRI study. *Cereb Cortex*. 19:1256–1262.

Buchwald M, Przybylski Ł, Kroliczak G. 2018. Decoding brain states for planning functional grasps of tools: a functional magnetic resonance imaging multivoxel pattern analysis study. *J Int Neuropsychol Soc*. 24:1013–1025.

Buckner RL, Andrews-Hanna JR, Schacter DL. 2008. The brain's default network. *Ann N Y Acad Sci*. 1124:1–38.

Buxbaum LJ, Randerath J. 2018. Limb apraxia and the left parietal lobe. *Handb Clin Neurol*. 151:349–363.

Buxbaum LJ, Shapiro AD, Coslett HB. 2014. Critical brain regions for tool-related and imitative actions: a componential analysis. *Brain*. 137:1971–1985.

Caspers S, Zilles K. 2018. Microarchitecture and connectivity of the parietal lobe. *Handb Clin Neurol*. 151:53–72.

Caspers S, Eickhoff SB, Geyer S, Scheperjans F, Mohlberg H, Zilles K, Amunts K. 2008. The human inferior parietal lobule in stereotaxic space. *Brain Struct Funct*. 212:481–495.

Caspers S, Eickhoff SB, Rick T, Kapri v A, Kuhlen T, Huang R, Shah NJ, Zilles K. 2011. Probabilistic fibre tract analysis of cytoarchitectonically defined human inferior parietal lobule areas reveals similarities to macaques. *Neuroimage*. 58:362–380.

Caspers S, Geyer S, Schleicher A, Mohlberg H, Amunts K, Zilles K. 2006. The human inferior parietal cortex: cytoarchitectonic parcellation and interindividual variability. *Neuroimage*. 33:430–448.

Choi SH, Na DL, Kang E, Lee KM, Lee SW, Na DG. 2001. Functional magnetic resonance imaging during pantomiming tool-use gestures. *Exp Brain Res*. 139:311–317.

Clower DM, Dum RP, Strick PL. 2005. Basal ganglia and cerebellar inputs to 'AIP. *Cereb Cortex*. 157:913–920.

Cole MW, Reynolds JR, Power JD, Repovs G, Anticevic A, Braver TS. 2013. Multi-task connectivity reveals flexible hubs for adaptive task control. *Nat Neurosci*. 16:1348–1355.

Constantino JN, Davis SA, Todd RD, Schindler MK, Gross MM, Brophy SL, Metzger LM, Shoushtari CS, Splinter R, Reich W. 2003. Validation of a brief quantitative measure of autistic traits: comparison of the social responsiveness scale with the autism diagnostic interview-revised. *J Autism Dev Disord*. 33:427–433.

Corbetta M, Patel G, Shulman GL. 2008. The reorienting system of the human brain: from environment to theory of mind. *Neuron*. 58:306–324.

D'Mello AM, Crocetti D, Mostofsky SH, Stoodley CJ. 2015. Cerebellar gray matter and lobular volumes correlate with core autism symptoms. *Neuroimage Clin*. 7:631–639.

DeMyer M, Alpern G, Barton S, DeMyer W, Churchill D, Hingtgen J, Bryson C, Pontius W, Kimberlin C. 1972. Imitation in autistic early schizophrenic and non-psychotic subnormal children. *J Autism Child Schizophr*. 2:264–287.

Desmurget M, Sirigu A. 2012. Conscious motor intention emerges in the inferior parietal lobule. *Curr Opin Neurobiol*. 22:1004–1011.

Desmurget M, Grafton S. 2000. Forward modeling allows feedback control for fast reaching movements. *Trends Cogn Sci*. 411:423–431.

Dewey D, Cantell M, Crawford SG. 2007. Motor and gestural performance in children with autism spectrum disorders developmental coordination disorder and/or attention deficit hyperactivity disorder. *J Int Neuropsychol Soc*. 132: 246–256.

Dixon ML, La Vega De A, Mills C, Andrews-Hanna J, Spreng RN, Cole MW, Christoff K. 2018. Heterogeneity within the frontoparietal control network and its relationship to the default and dorsal attention networks. *Proc Natl Acad Sci U S A* 1157:E1598–E1607.

Dowell LR, Mahone EM, Mostofsky SH. 2009. Associations of postural knowledge and basic motor skill with dyspraxia in autism: implication for abnormalities in distributed connectivity and motor learning. *Neuropsychologia*. 235:563–570.

Dziuk MA, Gidley Larson JC, Apostu A, Mahone EM, Denckla MB, Mostofsky SH. 2007. Dyspraxia in autism: association with motor social and communicative deficits. *Dev Med Child Neurol*. 4910:734–739.

Friston KJ, Penny WD, Glaser DE. 2005. Conjunction revisited. *Neuroimage*. 25:661–667.

Gonzalez Rothi LJ, Raymer AM, Heilman KM. 1997. Limb praxis assessment. In: Gonzales Rothi LJ, Heilman KM, editors. *Apraxia: The cognitive neuropsychology of praxis*. Hove: Psychology Press, pp. 61–74.

Grafton ST. 2009. Embodied cognition and the simulation of action to understand others. *Ann N Y Acad Sci*. 11561:97–117.

Hagmann P, Cammoun L, Gigandet X, Meuli R, Honey CJ, Wedeen VJ, Sporns O. 2008. Mapping the structural core of human cerebral cortex. *PLoS Biol*. 67:e159.

Hallett M, Lebiedowska MK, Thomas SL, Stanhope SJ, Denckla MB, Rumsey J. 1993. Locomotion of autistic adults. *Arch Neurol*. 50:1304–1308.

Hardwick RM, Caspers S, Eickhoff SB, Swinnen SP. 2018. Neural correlates of action: comparing meta-analyses of imagery, observation and execution. *Neurosci Biobehav Rev*. 94:31–44.

Haswell CC, Izawa J, Dowell LR, Mostofsky SH, Shadmehr R. 2009. Representation of internal models of action in the autistic brain. *Nat Neurosci*. 128:970–972.

Heilman KM, Gonzalez Rothi LJ. 2003. Apraxia. In: Valenstein E, editor. *Clinical neuropsychology*. 4th ed. New York: Oxford University, pp. 215–235.

Hermsdorfer J, Terlinden G, Muhlau M, Goldenberg G, Wohlschlager AM. 2007. Neural representations of pantomimed and actual tool use: evidence from an event-related fMRI study. *Neuroimage*. 36:109–118.

Hutchison RM, Culham JC, Flanagan JR, Everling S, Gallivan JP. 2015. Functional subdivisions of medial parieto-occipital cortex in humans and nonhuman primates using resting-state fMRI. *Neuroimage*. 116:10–29.

Igelström KM, Webb TW, Graziano MSA. 2015. Neural processes in the human temporoparietal cortex separated by localized independent component analysis. *J Neurosci*. 3525:9432–9445.

Igelström KM, Graziano MSA. 2017. The inferior parietal lobule and temporoparietal junction: a network perspective. *Neuropsychologia*. 105:70–83.

Igelström KM, Webb TW, Graziano MSA. 2017. Functional connectivity between the temporoparietal cortex and cerebellum in autism spectrum disorder. *Cereb Cortex*. 274:2617–2627.

Johnson-Frey SH, Newman-Norlund R, Grafton ST. 2005. A distributed left hemisphere network active during planning of everyday tool use skills. *Cereb Cortex*. 156:681–695.

Kroliczak G, Frey SH. 2009. A common network in the left cerebral hemisphere represents planning of tool use pantomimes and familiar intransitive gestures at the hand-independent level. *Cereb Cortex*. 1910:2396–2410.

Kroliczak G, Piper BJ, Frey SH. 2016. Specialization of the left supramarginal gyrus for hand-independent praxis representation is not related to hand dominance. *Neuropsychologia*. 93:501–512.

Lau WKW, Leung M-K, Lau BWM. 2019. Resting-state abnormalities in autism spectrum disorders: a meta-analysis. *Sci Rep*. 9:3892.

Leech R, Sharp DJ. 2014. The role of the posterior cingulate cortex in cognition and disease. *Brain*. 1371:12–32.

Leiguarda RC, Marsden CD. 2000. Limb apraxias: higher-order disorders of sensorimotor integration. *Brain*. 123:860–879.

Lynch CJ, Uddin LQ, Supekar K, Khouzam A, Phillips J, Menon V. 2013. Default mode network in childhood autism: posteromedial cortex heterogeneity and relationship with social deficits. *Biol Psychiatry*. 743:212–219.

MacNeil LK, Mostofsky SH. 2012. Specificity of dyspraxia in children with autism. *Neuropsychology*. 262:165–171.

Marko MK, Crocetti D, Hulst T, Donchin O, Shadmehr R, Mostofsky SH. 2015. Behavioural and neural basis of anomalous motor learning in children with autism. *Brain*. 1383: 784–797.

Mattar MG, Cole MW, Thompson-Schill SL, Bassett DS. 2015. A functional cartography of cognitive systems. *PLoS Comput Biol*. 11:e1004533.

McAuliffe D, Pillai AS, Tiedemann A, Mostofsky SH, Ewen JB. 2016. Dyspraxia in ASD: impaired coordination of movement elements. *Autism Res*. 10:648–652.

Moher Alsady T, Blessing EM, Beissner F. 2016. MICA-A toolbox for masked independent component analysis of fMRI data. *Hum Brain Mapp*. 3710:3544–3556.

Morecraft RJ, Cipolloni PB, Stilwell-Morecraft KS, Gedney MT, Pandya DN. 2003. Cytoarchitecture and cortical connections of the posterior cingulate and adjacent somatosensory fields in the rhesus monkey. *J Comp Neurol*. 4691:37–69.

Mostofsky SH, Ewen JB. 2011. Altered connectivity and action model formation in autism is autism. *Neuroscientist*. 174:437–448.

Mostofsky SH, Dubey P, Jerath VK, Jansiewicz EM, Goldberg MC, Denckla MB. 2006. Developmental dyspraxia is not limited to imitation in children with autism spectrum disorders. *J Int Neuropsychol Soc*. 123:314–326.

Mostofsky SH, Powell SK, Simmonds DJ, Goldberg MC, Caffo B, Pekar JJ. 2009. Decreased connectivity and cerebellar activity in autism during motor task performance. *Brain*. 1329:2413–2425.

Nebel MB, Eloyan A, Nettles CA, Sweeney KL, Ament K, Ward RE, Choe AS, Barber AD, Pekar JJ, Mostofsky SH. 2016. Intrinsic visual-motor synchrony correlates with social deficits in autism. *Biol Psychiatry*. 798:633–641.

Oberman LM, Ramachandran VS. 2007. The simulating social mind: the role of the mirror neuron system and simulation in the social and communicative deficits of autism spectrum disorders. *Psychol Bull*. 133:310–327.

Parlatini V, Radua J, Dell'Acqua F, Leslie A, Simmons A, Murphy DG, Catani M, Thiebaut de Schotten MT. 2017. Functional segregation and integration within fronto-parietal networks. *Neuroimage*. 146:367–375.

Parvizi J, Van Hoesen GW, Buckwalter J, Damasio A. 2006. Neural connections of the posteromedial cortex in the macaque. *Proc Natl Acad Sci U S A* 1035:1563–1568.

Pitzalis S, Fattori P, Galletti C. 2012. The functional role of the medial motion area V6. *Front Behav Neurosci*. 6:91.

Prevosto V, Graf W, Ugolini G. 2010. Cerebellar inputs to intraparietal cortex areas LIP and MIP: functional frameworks for adaptive control of eye movements reaching and arm/eye/-head movement coordination. *Cereb Cortex*. 201:214–228.

Ptak R, Schnider A, Fellrath J. 2017. The dorsal frontoparietal network: a core system for emulated action. *Trends Cogn Sci*. 218:589–599.

Quallo MM, Price CJ, Ueno K, Asamizuya T, Cheng K, Lemon RN, Iriki A. 2009. Gray and white matter changes associated with tool-use learning in macaque monkeys. *Proc Natl Acad Sci USA*. 106:18379–18384.

Rizzolatti G, Rozzi S. 2018. The mirror mechanism in the parietal lobe. *Handb Clin Neurol*. 151:555–573.

Scheperjans F, Eickhoff SB, Homke L, Mohlberg H, Hermann K, Amunts K, Zilles K. 2008. Probabilistic maps morphometry and variability of cytoarchitectonic areas in the human superior parietal cortex. *Cereb Cortex*. 189:2141–2157.

Skefos J, Cummings C, Enzer K, Holiday J, Weed K, Levy E, Yuce T, Kemper T, Bauman M. 2014. Regional alterations in purkinje cell density in patients with autism. *PLoS One*. 92:e81255–e81212.

Spreng RN, Mar RA, Kim ASN. 2009. The common neural basis of autobiographical memory prospection navigation theory of mind and the default mode: a quantitative meta-analysis. *J Cogn Neurosci*. 213:489–510.

Stoodley CJ, D'Mello AM, Ellegood J, Jakkamsetti V, Liu P, Nebel MB, Gibson JM, Kelly E, Meng F, Cano CA *et al*. 2017. Altered cerebellar connectivity in autism and cerebellar-mediated

rescue of autism-related behaviors in mice. *Nat Neurosci*. 20:1744–1751.

Teitelbaum P, Teitelbaum O, Nye J, Fryman J, Maurer RG. 1998. Movement analysis in infancy may be useful for early diagnosis of autism. *Proc Natl Acad Sci U S A*. 95:13982–13987.

Vincent JL, Kahn I, Snyder AZ, Raichle ME, Buckner RL. 2008. Evidence for a frontoparietal control system revealed by intrinsic functional connectivity. *J Neurophysiol*. 1006: 3328–3342.

Welner Z, Reich W, Herjanic B, Jung KG, Amado H. 1987. Reliability validity and parent-child agreement studies of the Diagnostic Interview for Children and Adolescents: DICA. *J Am Acad Child Adolesc Psychiatry*. 26:649–653.

Whitney ER, Kemper TL, Bauman ML, Rosene DL, Blatt GJ. 2008. Cerebellar purkinje cells are reduced in a subpopulation of autistic brains: a stereological experiment using calbindin-D28k. *Cerebellum*. 7:406–416.

Wiestler T, Diedrichsen J. 2013. Skill learning strengthens cortical representations of motor sequences. *Elife*. 2:e00801.

Wymbs NF, Grafton ST. 2015. The human motor system supports sequence-specific representations over multiple training-dependent timescales. *Cereb Cortex*. 2511:4213–4225.